



Mechanical behavior of wood subjected to mode II fracture, using an energetic criterion: Application on THUJA of Morocco

Amal Saoud, Abdelhamid Elamri, Khadija Kimakh, M'hamed Chergui

University of Hassan II, National Superior School of Electricity and Mechanics Casablanca (ENSEM), LCCMMS, Morocco.

Saoudamal22@gmail.com <http://orcid.org/0000-0002-2139-2627>

Khadija.kimakh@gmail.com <http://orcid.org/0000-0002-2418-1307>

Mohsine Ziani

Institut National des Sciences de l'Archéologie et du Patrimoine (INSAP)/Rabat, Morocco.

Moussa Elmatar

Centre Technique d'Industrie du Bois et d'Ameublement (CTIBA)/Casablanca, Morocco.



ABSTRACT. Shear strength is one of the properties often used to qualify a wood species for use in industry. But until now there is no standardized test which allows understanding this phenomenon. This paper constitutes a new approach to study the behavior of the wood material subjected to the mode II fracture. For that we designed and realized a new prototype of a wooden specimen that we tested in our laboratory which gives rise to an evaluation of the fracture until separation by pure shear of the specimen in the TL plane. The experimental data from a first series of tests on Thuja wood (*Tetraclinis Articulata* (Vahl) Masters) as a test material as well as the calculation of mode II initiation fracture toughness and the critical stress intensity factor are presented in this paper.

KEYWORDS. Shear; Mode II fracture; *Tetraclinis Articulata*; Moroccan Thuja Wood; Experimental testing.

Citation: Saoud, A., Elamri, A., Kimakh, K., Chergui, M., Ziani, M., Elmatar, M., Mechanical behavior of wood subjected to mode II fracture, using an energetic criterion: Application on THUJA of Morocco, *Frattura ed Integrità Strutturale*, 44 (2018) 25-34.

Received: 16.09.2017

Accepted: 15.01.2018

Published: 01.04.2018

Copyright: © 2018 This is an open access article under the terms of the CC-BY 4.0, which permits unrestricted use, distribution, and reproduction in any medium, provided the original author and source are credited.

INTRODUCTION

At the beginning of the 21st century, environmental issues require the special attention of researchers. The process of transformation of wood has been proved to be the least expensive in terms of energy. The study of the mechanical behavior of wood is rising especially after recommendations following the conference of parties (COP): Kyoto, Rio, Paris and Marrakech. It is for this reason that the environmental commitments of the participating countries further stimulate scientific research on wood material for a more massive use in the context of reasonable logging.



The study of this heterogeneous material requires knowledge of its behavior in the face of different solicitations, while knowing that wood as a natural material contains many defects, the application of the theory of fracture mechanics, which is a mean of estimating the stability of cracks in the immediate vicinity of the defects, is essential. It also makes it possible to predict the critical propagation length as a function of the loading applied. Accordingly, it is fundamental to provide accurate measurements of the fracture properties such as initiation fracture toughness under Mode I, Mode II, Mixed mode I + II and Mode III.

The mode I fracture has been widely studied by different researchers using several types of standard specimens namely: compact tension (CT), single-edge notched tension (SENT), double-edge notched tension (DENT), single-edge notched three-point Bending (SEN3B) tests [1-5] and the Double Cantilever Beam (DCB). Concerning the DCB test specimen, its efficiency has been universally accepted thanks to its simplicity of design and realization for the measurement of toughness (G_{IC} and K_{IC}) by the simple beam theory [6]. Wood fracture behavior under shear is one of the phenomena until now not fully controlled, that is why several prototypes have been proposed to approach closely the nature of the fracture in mode II of rupture, the three main tests are based on flexure: the most commonly used test is the End-Notched Flexure (ENF) which is a beam-like test specimen containing an artificial crack on one side and is loaded under three-point bending. The application of the load is rather simple, the propagation of the crack from the initial crack is unstable except for the very large notch lengths $a/L > 0.7$ [7]. Studies using ENF have been performed with an a/L ratio of 0.5 [8-10], so the propagation is unstable.

Other researchers use End Loaded Split (ELS) [11]: The sound side of a prismatic/beam specimen is clamped while the side containing the artificial defect is loaded in the direction of thickness. The loading is generally applied to the test specimen via a load block. The ELS test makes it possible to obtain a stable crack propagation in mode II if the condition $a/L > 0.55$ is respected [7]. Nevertheless, it requires a rather complicated assembly to maintain the boundary conditions.

Finally, there is the most recent 4-Point Bend End-Notched Flexure (4ENF) test specimen: a specimen containing an artificial defect on one side and loaded under four-point bending; this prototype has the advantage of being the most stable, but the acquisition of results requires sophisticated equipment.

In this paper, a new test prototype is presented which is easy to use and stable and in which the rupture of the specimen can be perceived under mode II.

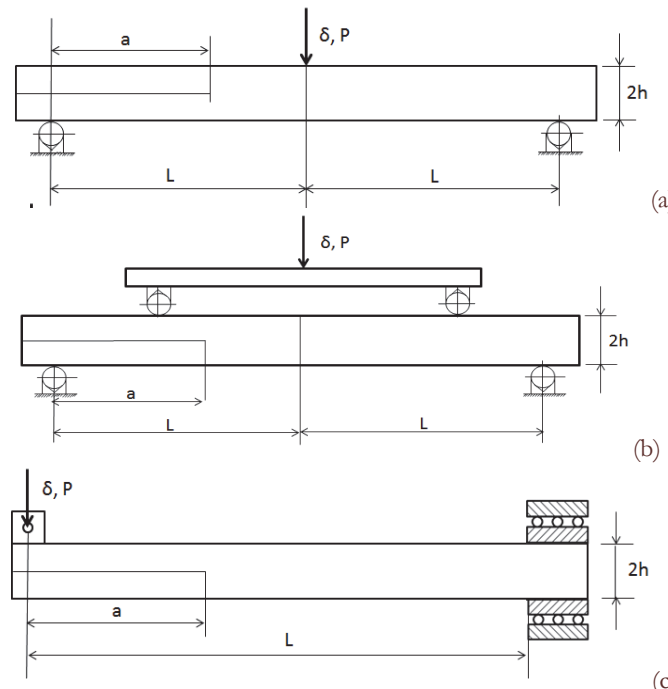


Figure 1: Mode II test configurations. (a) End notched flexure (ENF), (b) four-point end notched flexure (4ENF) and (c) End Loaded Split (ELS).

MATERIAL AND METHODS

The experimental work consisted in subjecting thin, notched flat specimens with different cut lengths to Mode II tensile tests. All specimens and the gripping device were specially designed and produced for the purpose of this research.

Test material

The material used is Moroccan Thuja "Tectracanalis Articulata" from the Middle Atlas plateau (Khemissat region). In Morocco, Thuja occupies a total area of about 680 000 ha (equivalent to 11.7% of the total area covered by the Moroccan forest) and plays an important socioeconomic role in the satisfaction of Local needs of riparian populations for rangelands, firewood and various service woods [12]. These trees have no defects or rot. By respecting the various dimensions according to the specificities of the test, the test specimens were made from 25 mm thick ridges. In order to better characterize the material, physical and mechanical characterization tests.

- Physical measurements

The moisture, the densities and the shrinkage along the three axes are determined on cubic specimens (20 mm × 20 mm × 20 mm) respectively according to standards NF B 51-004, NF B 51-005 and NF B 51-006.

- Mechanical measurements

The longitudinal elastic modulus E_l and the static flexural strength σ_{fs} were determined by 4-point bending tests using prismatic specimens of (20 mm × 20 mm × 360 mm) cut aligned to the three symmetry directions of the wood in compliance with standard NF B51-008. Compression tests were carried out to determine the stress at break σ_a according to the NF B 51-007 standard and finally shear tests on test pieces whose dimensional specificities are detailed in standard NF B 51-012 were also performed to evaluate the longitudinal shear strength, R_{Lc} .

	d_H g/cm ³	d_0 g/cm ³	$R_v(%)$	$R_T(%)$	$R_R(%)$	Anisotropy	E_l (MPa)	σ_a (MPa)	σ_{fs} (MPa)	R_{Lc} (MPa)
Average	0.68	0.63	4.98	2.9	1.83	0.64	7437	35	82.22	30
Standard deviation	0.03	0.02	0.46	0.45	0.06	0.11	148.1	0.38	25.93	2.41

d_H : density of the specimen in the moisture state H, d_0 : density of the specimen in the anhydrous state, $R_v(%)$:volumetric shrinkage , $R_T(%)$:tangential shrinkage , $R_R(%)$:radial shrinkage, E_l : Longitudinal Young's modulus, σ_a : compressive stress σ_{fs} : static bending strength R_{Lc} : Longitudinal shear strength.

Table 1: Main physical and mechanical characteristics of Thuja.

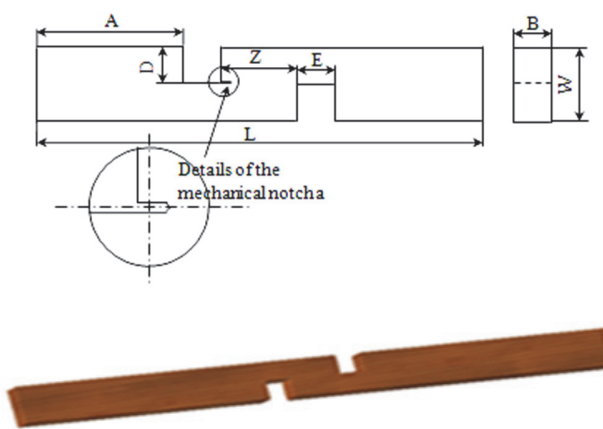


Figure 2: Representation of the test specimen.



- Prototype of the fracture specimen designed

The fracture specimens used were made from logs of *Thuja* trees from the plateau of the Middle Atlas of Morocco. These specimens are intended for crack propagation under mode I+II but dominated by mode II. Fig. 2 illustrates the geometry and dimensional characteristics are presented in Tab. 2.

Symbol	Description	Dimensions (mm) accuracy of $\pm 0.1\text{mm}$
W	Width of the specimen	20
B	Thickness of the specimen	10
E	The width of the groove	10
D	The depth of the groove	10
L	Length of the specimen	234
Z	The area of damage	20
a	Length of notch	$6 \leq a \leq 12$
A	Gripping area	97

Table 2: Dimensional characteristics of the fracture specimen.

- Principle of the test

The specimens are provided by a mechanical cut made using a jigsaw. A suitable device has been set up to have a precise notch depth and to ensure a displacement parallel to the base plane of the groove; the details of this mechanical notch are shown in Fig. 3.

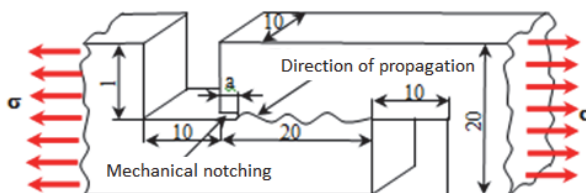


Figure 3: Representation of the proposed test specimen.

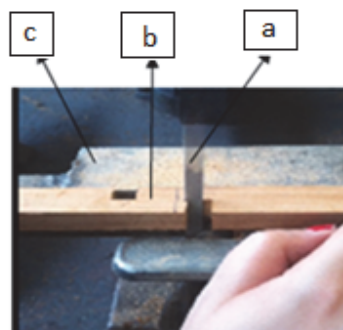


Figure 3: Realization of the notch with (a) blade 1 mm thick, (b) test specimen for mode II fracture characterization and (c) slip gauge.

This operation was reproduced on twenty-five specimens that were placed in a climatic chamber at a temperature of 10°C and 74% of humidity until material stabilization at moisture content of 15%. Before each test, a razor blade was used to increase the sharpness of the mechanical notch, granting consistency with the Linear Fracture Mechanics.

- Conduction of tests

The test specimens were placed in a universal test machine type "MTS 810", which allows the conduction of controlled tensile tests. This machine is equipped with a computer with control software which gives the recordings of the variation of the applied load as a function of the spacing of the lips of the crack for each specimen under test. This applied load is

measured by the load cell installed on the upper cross-member of the machine. Load-displacement records are viewed on a computer screen and then stored for analysis.

The two ends of the test specimen are then introduced into the gripping device as illustrated in Fig. 4.

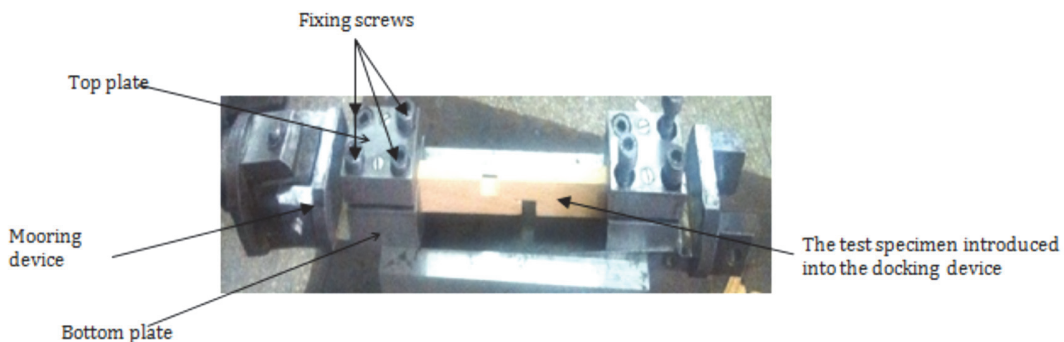


Figure 4: Gripping device.

The gripping device uses two ball-joints to ensure the alignment between the axis of the cross-member and that of the jack. The assembly has been placed in the tensile machine shown in the Fig. 5.

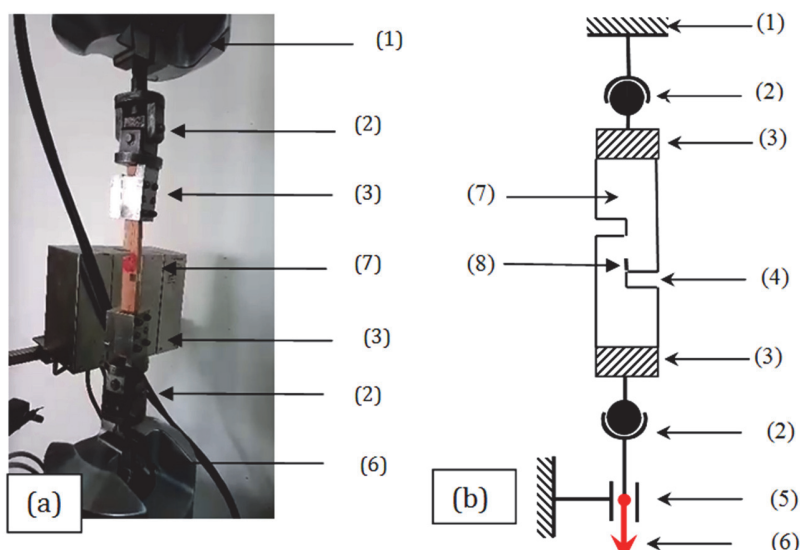


Figure 5: (a) Photo of mounted test specimen, (b) kinematic diagram of the test specimen mounted in the gripping device: (1) machine jaws; (2) ball joint connection; (3) gripping area; (4) grooves; (5) pivot pin; (6) loading direction; (7) test specimen; (8) mechanical notch.

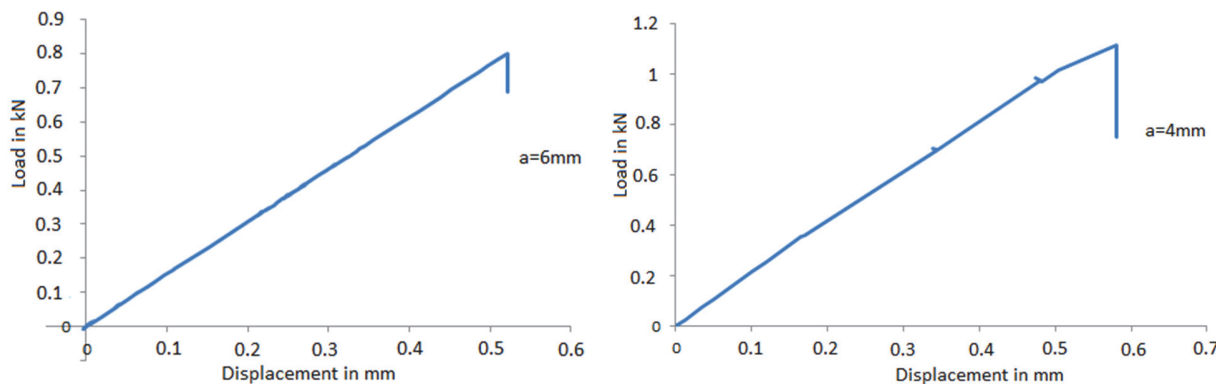
The testing machine allowed the application of an axial tensile force parallel to the wood grain on a series of 25 test specimens with a constant speed of 0.5 mm/min. This loading allowed the propagation of the crack until a shear rupture surface was created.

RESULTS AND DISCUSSION

The experimental results of a test carried out under the same conditions are presented in the following.

Force-displacement curves

Fig. 6 illustrates typical force/displacement curves.

Figure 6: Load-displacement curves for $a = 6\text{mm}$ and $a=4\text{mm}$.

The behaviour of our test piece during the test can be qualified as elastic under the action of the applied load. Fig. 6 shows the superposition of the load / displacement curve obtained for Thuja wooden specimens. It is noted that the crack propagates linearly until reaching the maximum load. It is also noted that the curve experiences oscillations during loading which can be explained by heterogeneities of wood, internal defects, variability in growth rings. Cracks tend to propagate in growth rings corresponding to early wood (low intensity). To ensure the validity of our results and to consider the scatter, the tests were carried out on batches of 25 test pieces, taking care to distribute them in five small batches of five test pieces each with a notch length a ($a = 4, 6, 8, 10, 12 \text{ mm}$). Fig. 7 shows the load-displacement curves for different initial crack sizes of the test specimens tested. With a constant test speed of $0.5 \text{ mm} / \text{min}$ as previously reported, the average tensile load decreases as the crack length increases as shown in Tab. 3.

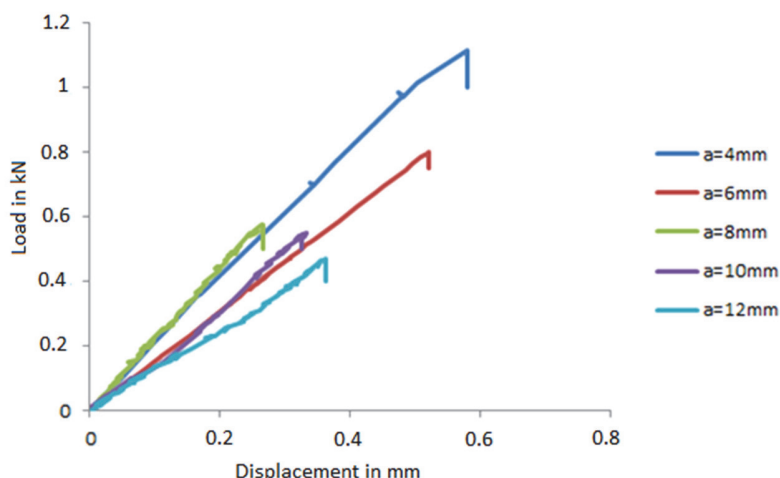


Figure 7: The load-displacement curves for the different lengths of initial notches.

It is noted that the maximum loads vary from one test to another with the same notch length and under the same conditions; a normal thing due to the high heterogeneity of the wood material but the appearance of the curves remains consistent.

The G_{IIC} mode II initiation fracture toughness and the K_{IIC} stress intensity factor of the Thuja massive wood.

Experimental approach has helped to determine two important parameters, namely the strain energy release rate and the stress intensity factor. To do this, we started by determining the compliance as a function of the crack size. The set of load-displacement curves provides several values of the compliance C_i (a_i), defined by the slope of the load-displacement curve $C = \delta/P$ (see Fig. 8), where δ and P represent the displacement and the applied load, respectively. The experimental points were smoothed using a polynomial of order 3.

	Crack length a (mm)	Critical load (kN)	Average load (kN)	Standard deviation (kN)
a=4	1			
	0.81			
	1.14	0.95		0.13
	0.98			
a=6	0.80			
	0.882			
	1			
	0.90	0.88		0.07
a=8	0.85			
	0.801			
	0.57			
	0.59			
a=10	0.60	0.59		0.01
	0.60			
	0.57			
	0.54			
a=12	0.54	0.55		0.01
	0.55			
	0.57			
	0.51			
a=12	0.40			
	0.47	0.51		0.07
	0.54			
	0.61			

Table 3: Evolution of the maximum load for each test.

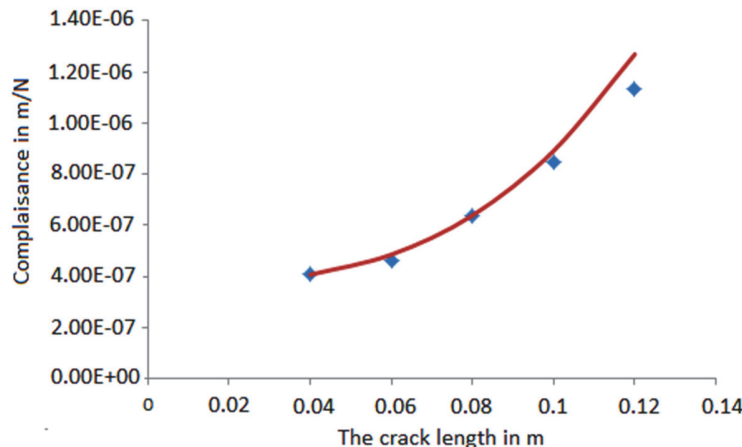


Figure 8: The experimentally defined compliance as a function of the crack length.

To perform the calculations, the following assumptions were assumed:

- Wood is a homogeneous material because the dimensions of the specimen are large compared to the difference between the diameters of two consecutive rings.
- The elastic behavior is valid.
- The orthotropic stiffness matrix is known.
- The elastic constants used hereinafter, listed in Tab. 4, were determined using the predictive model developed by



- Guitard, knowing that the density of wood is $d = 0.60 \text{ g / cm}^3$ [14]. To facilitate the comparison of results with the literature, while knowing that almost most researchers in this component uses this database.

S_{11}^{-1} (MPa)	S_{22}^{-1} (MPa)	S_{33}^{-1} (MPa)	S_{12}^{-1} (MPa)	S_{23}^{-1} (MPa)	S_{31}^{-1} (MPa)	S_{44}^{-1} (MPa)	S_{55}^{-1} (MPa)	S_{66}^{-1} (MPa)
1355.5	922.5	19355	2842	45950	51750	893.35	1173	117.8

S_{ij} : The components of the compliance matrix which are in function of the elastic constants of the wood

Table 4: Elastic constants of Thuja.

- The GIIC mode II initiation fracture toughness.

G , the initiation fracture toughness corresponding to a small crack increment can be computed using the analytical form according to IRWIN-KIES [6]:

$$G_{II} = \frac{P^2}{2B} \frac{\partial C}{\partial a} \quad (1)$$

where B is the thickness of the specimen; P is the applied load and a the crack length.

$$G_{IIC} = \left. \frac{P_c^2}{2B} \frac{\partial C}{\partial a} \right|_{a=a_c} \quad (2)$$

The critical value of G_{II} , G_{IIC} , is then found by measuring the critical load P_c needed to fracture a specimen containing a crack of length a_c , and using the slope of the compliance curve at this same value of a [13] :

We note that:

$$C = ma^3 + C_0 \quad (3)$$

Where m and C_0 are determined by a linear regression of the experimental curve C as a function of a^3

The critical stress intensity factor K_{IIC}

Mode II initiation fracture toughness G_{II} and stress intensity factor K_{II} , assuming elastic linear behavior, are related to each other. The relationship between these two quantities is obtained using the following equation [14]:

$$G_{IIC} = \frac{K_{IIC}^2 S_{11}}{\sqrt{2}} \left[\left(\frac{S_{22}}{S_{11}} \right)^{\frac{1}{2}} + \frac{(2S_{12} + S_{66})}{2S_{11}} \right]^{\frac{1}{2}} \quad (4)$$

a (mm)	G_{II} N/m		K_{II} MPa. \sqrt{m}	
	Mean value	Standard deviation	Mean value	Standard deviation
4	113.95	33.37	0.40	0.06
6	221.99	37.14	0.56	0.05
8	174.65	9.20	0.50	0.05
10	237.20	11.87	0.58	0.05
12	267.06	62.51	0.61	0.02

Table 5: Mode II initiation fracture toughness and corresponding stress intensity factors.



We set the mean value of the Mode II initiation fracture toughness G_{IIC} and the K_{IIC} critical stress intensity factor determined using respectively the formulas cited previously in (3) and (4) in Tab. 5. Knowing that a material subjected to stresses contains stored elastic energy stored, during material cracking, there is an energy release.

In Fig. 9 a dispersion is observed for each value of a , except for the values of 8 and 10 mm, this dispersion is less visible. It is also observed that the propagation of the crack is stable from the ratio $a=6\text{mm}$. Hence a quasi-stability of our prototype, we can conclude that for values greater than $a / W = 0.3$ G_{II} and K_{II} , are a characteristic of the wood material.

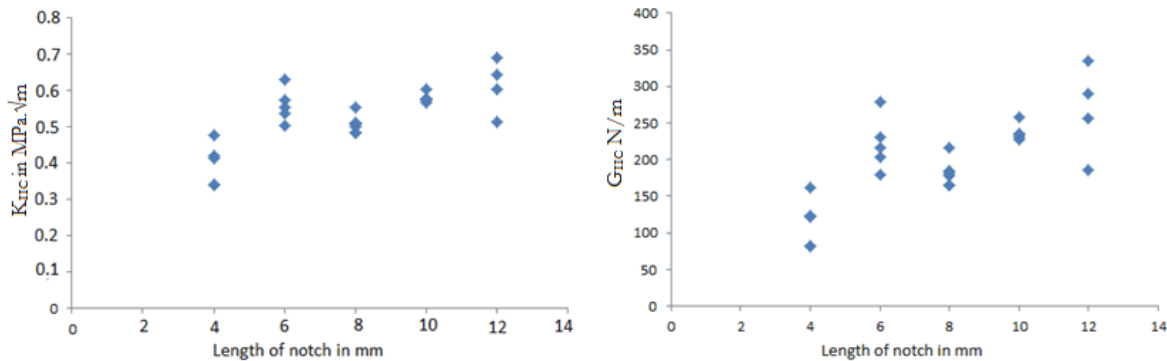


Figure 9: Evolution of the energy restitution rate G_{II} and K_{II} as a function of the crack length.

We cannot conclude without comparing our results with the literature. However, the wood has a lot of inter and intra-tree dispersal; moreover the moisture rate and the conditions in which the tests were carried out have a great influence on the results. We can only compare orders of magnitude. In Tab. 6 we compare our results with the literature.

Specimens	Wood Species	Reference	G_{IIC}
ELS	Pinus pinaster	[11]	0.319
ENF	Pinus pinaster	[16]	0.637
3ENF	Stika Spruce	[10]	0.39
Our work	Thuya of Morocco		0.202

Table 6: The comparative table of our results with the literature.

CONCLUSION

A new test method for the study of the behavior of wood material subjected to a shear stress in the longitudinal plane was developed. The experimental protocol of this test was applied to a first series of a resinous species: Thuja of Morocco. We were able to determine G_{IIC} and K_{IIC} from the typical recording of the load-displacement curve during the stable propagation of the crack and using the method of complacency. These results were compared with the literature where it was observed that our approach presents an ease in the production and application of the specimens for mode II propagation. Unlike other devices previously presented the comparison of the results shows a high consistency.

REFERENCES

- [1] Schniewind, A.P. and Pozniak, R.A. (1971). On the fracture toughness of Douglas-fir wood, Engineering Fracture Mechanics, 2, pp. 223-230. DOI: 10.1520/ACEM20120045.
- [2] Mall, S., Murphy, J.F. and Shottaffer, J.E. (2016). Criterion for mixed mode fracture in wood. Materials Science and Engineering: A, 527, pp. 27–28. DOI: 10.1016/j.msea.2010.08.004.
- [3] Triboullet, P., Jodin, P. and Pluvinage, G. (1984). Validity of fracture mechanics concepts applied to wood by finite element calculation, Wood Sci Technol, 18, pp. 51–58. DOI: 10.1007/BF00632130.



- [4] Kretschmann, D.E. and Green, D.W. (1985). Modeling moisture content mechanical property relationships for clear southern pine. *Wood Fiber science*.
- [5] King, M.J., Sutherland, I.J. and Le-Ngoc, L. (1995). Fracture toughness of wet and dry Pinus radiata, *European Journal of wood and wood product*, 57, pp. 235–240. DOI: 10.1007/s001070050 .
- [6] Dourado, N., Morel, S., de Moura, M.F.S.F., Valentin, G. and Morais, J. (2008). Comparison of fracture properties of two wood species through cohesive crack simulations, *Composites Part A*, 39, pp. 415-427. DOI: 10.1016/j.compositesa.2007.08.025.
- [7] Yoshihara, H. (2007). Simple estimation of critical stress intensity factors of wood by tests with double cantilever beam and three-point end notched flexure. *Holzforschung*, 61, pp. 182–189. DOI: 10.1515/HF.2007.032 .
- [8] Davies, P., Blackman, B.R.K. and Brunner (1998). Standard test methods for delamination resistance of composite materials, *Applied Composite Materials*, 5, pp.345. DOI 10.1023/A:1008869811626.
- [9] Davies, P., Blackman, B.R.K. and Brunner, A.J. (2001).Mode II delamination. European Structural Integrity Society, 28, pp. 307-333. DOI: 10.1016/S1566-1369(01)80039-X.
- [10] Silva, M.A.L., de Moura, M.F.S.F. and Morais, J.J.L. (2006). Numerical analysis of the ENF test for mode II wood fracture *Composites Part A*, 37, pp. 1334–1344.DOI: 10.1016/j.compositesa.2005.08.014.
- [11] Yoshihara, H. and Ohta, M. (2000). Measurement of mode II fracture toughness of wood by the end-notched flexure test, *J Wood Sci*, 46, pp. 273. DOI:10.1007/BF00766216.
- [12] Silva, M.A.L., Morais, J.J.L., de Moura, M.F.S.F. and Lousada, J.L. (2007) Mode II wood fracture characterization using the ELS test.*Engineering Fracture Mechanics*, 74, pp. 2133-2147 DOI: /10.1016/j.engfracmech.2006.10.012 .
- [13] Ellatif, M. (2012). L'économie de la forêt et des produits forestiers au Maroc: Bilan et Perspectives.
- [14] Roylance, D. (2001). Introduction to Fracture Mechanics, Department of Materials Science and Engineering Massachusetts Institute of Technology Cambridge, MA 02139.
- [15] Guitard, D. and El Amri, F., (1987). Modèles prévisionnels de comportement élastique tridimensionnel pour les bois feuillus et les bois résineux, *Annals of Forest Science*, 44, pp. 335-358. DOI: 10.1051/forest:19870305.
- [16] Yoshihara, H. (2005). Mode II initiation fracture toughness analysis for wood obtained by 3-ENF test *Composites Science and Technology*, 65, pp. 2198-2207 DOI: 10.1016/j.compscitech.2005.04.019.